

MOL #29108

Synergistic Neuroprotection by Bis(7)-tacrine via Concurrent Blockade of N-Methyl-D-aspartate Receptors and Neuronal Nitric Oxide Synthase

Wenming Li, Jian Xue, Chunying Niu, Hongjun Fu, Colin S.C. Lam, Jialie Luo, Hugh H.N. Chan, Huaiguo Xue, Kelvin K.W. Kan, Nelson T.K. Lee, Chaoying Li, Yuanping Pang, Mingtao Li, Karl W.K. Tsim, Hualiang Jiang, Kaixian Chen, Xiaoyuan Li and Yifan Han

Departments of Biochemistry (W.L., H.F., C.S.C.L., J.L., H.H.N.C., K.K.W.K., N.T.K.L., Y.H.), Chemistry (J.X., H.X., X.L.) and Biology (K.W.K.T.), Hong Kong University of Science and Technology, Hong Kong; Center for Drug Discovery and Design, State Key Laboratory of Drug Research, Shanghai Institute of Materia Medica, Shanghai 201203, China (C.N., H.J., K.C.); Laboratory of Molecular and Cellular Neurobiology, National Institute on Alcohol Abuse and Alcoholism, National Institutes of Health, Bethesda, Maryland 20892 (C.L.); Mayo Foundation for Medical Education and Research, Rochester, Minnesota 55905 (Y.P.) and Department of Pharmacology and Proteomics Lab, Zhongshan Medical College, Sun Yat-sen University, Guangzhou 510080, China (W.L., M.L.)

MOL #29108

Running Title:

Neuroprotection by Bis(7)-tacrine via Dual Targets

Corresponding Author:

Dr. Yifan Han, Associate Professor. Department of Biochemistry, Hong Kong University of Science and Technology, Clear Water Bay, Kowloon, Hong Kong SAR, China.

Tel.: 852-23587293; Fax: 852-23581552; E-mail: bcyfhan@ust.hk

Number of Each Item:

Text pages: **26**

Tables: **3**

Figures: **5**

References: **35**

Abstract: **247** words

Introduction: **607** words

Discussion: **1467** words

List of Abbreviations:

AChE, acetylcholinesterase; AD, Alzheimer's disease; ANOVA, analysis of variance; CGNs, cerebellar granule neurons; e/i/nNOS, endothelial/inducible/neuronal NO synthase; L-NMMA, N^G-monomethyl-L-arginine; MTT, 3(4,5-dimethylthiazol-2-yl)-2,5-diphenyltetrazolium bromide; NMDA(R), N-methyl-D-aspartate (receptor); NO, nitric oxide.

MOL #29108

ABSTRACT

The excessive activation of the N-methyl-D-aspartate receptor (NMDAR)/nitric oxide (NO) pathway has been proposed to be involved in the neuropathology of various neurodegenerative disorders. In this study, NO was found to mediate glutamate-induced excitotoxicity in primary cultured neurons. Compared with the NO synthase (NOS) inhibitor, N^G-monomethyl-L-arginine (L-NMMA), and the NMDAR antagonist memantine, bis(7)-tacrine was found to be more potent in reducing NO-mediated excitotoxicity and the release of NO caused by glutamate. Moreover, like L-NMMA but not like MK-801 and memantine, bis(7)-tacrine showed greater neuroprotection and inhibition on NO release when neurons were pretreated for a prolonged time between 0 and 24 h, and remained quite potent even when neurons were post-treated 1 h after the glutamate challenge. Bis(7)-tacrine was additionally found to be as moderately potent as memantine in competing with [³H]MK-801, inhibiting NMDA-evoked currents and reducing glutamate-triggered calcium influx, which eventually reduced neuronal NOS activity. More importantly, at neuroprotective concentrations, bis(7)-tacrine substantially reversed the overactivation of neuronal NOS caused by glutamate without interfering with the basal activity of NOS. Furthermore, *in vitro* pattern analysis demonstrated that bis(7)-tacrine competitively inhibited both purified neuronal and inducible NOS with IC₅₀ at 2.9 and 9.3 μM but not endothelial NOS. This result was further supported by molecular docking simulations that showed hydrophobic interactions between bis(7)-tacrine and three NOS isozymes. Taken together, these results strongly suggest that the substantial neuroprotection against glutamate by bis(7)-tacrine might be mediated synergistically through the moderate blockade of NMDAR and selective inhibition of neuronal NOS.

MOL #29108

INTRODUCTION

The precise mechanisms leading to the pathogenesis of chronic and acute neurodegenerative disorders have not yet been fully elucidated. However, increasing evidence has shown that these diseases may share a final common pathway to neuronal injury due to the excitotoxicity caused by the overstimulation of glutamate receptors of the N-methyl-D-aspartate (NMDA) subtype (Sonkusare et al., 2005; Yuan and Yankner, 2000). Excessive nitric oxide (NO), generated by neuronal NO synthase (nNOS), which is tethered to the NMDA receptor (NMDAR) and activated by Ca^{2+} over-influx via the receptor-associated ion channel, mediates the downstream signal transduction of the NMDAR (Lipton, 2004; Yamauchi et al., 1998) and leads to the excitotoxic neuronal cell death (Boje, 2004; Lipton, 2004). Given the role that NMDAR/NO signaling plays during the development and progression of various neurodegenerative diseases, reducing excessive NO generation by directly/indirectly inhibiting nNOS may be an excellent strategy for preventing and treating neurodegenerative disorders (Fedorov et al., 2004; Grunewald and Beal, 1999; Lipton, 2004). Actually, the use of NMDAR antagonists for neurodegenerative diseases has been realized in the use of memantine (a moderate antagonist of NMDAR) in successful treatment of moderate to severe Alzheimer's disease (AD) (Sonkusare et al., 2005); additionally, several nNOS inhibitors such as 7-nitroindazole (7-NI) and ARL17477 have been demonstrated as promising candidates for treating other neurodegenerative diseases such as stroke (Lipton, 2004; Willmot et al., 2005).

On the other hand, since multi-factorial etiopathogenesis is clearly indicated in neurodegenerative disorders, multiple drug therapy is required to address the varied pathological aspects of these diseases (Mattson, 2004). Current approaches with one-drug-one-target only offer limited and transient benefits to patients but do not significantly delay the course of

MOL #29108

neurodegeneration (Frantz, 2005; Youdim et al., 2005). Multi-functional compounds might provide greater therapeutic efficacy by targeting different sites in the brain concurrently (Van der Schyf et al., 2006; Zhang, 2005). Therefore, new one-drug-multiple-targets approaches have been developed expressly to target multiple sites in the central nervous system with single molecular entities for the treatment of these diseases (Youdim et al., 2005; Zhang, 2005).

Over the past few years, we have demonstrated that bis(7)-tacrine, a dimeric acetylcholinesterase (AChE) inhibitor, may be a multi-functional entity with the following properties. Briefly, bis(7)-tacrine has been reported as a promising therapeutic agent for AD on the basis of its AChE inhibition (Pang et al., 1996; Wang et al., 1999) and superior memory-enhancement capabilities (Liu et al., 2000). Moreover, bis(7)-tacrine protects against ischemia-induced injury in mouse astrocytes (Wu et al., 2000) and hydrogen peroxide-induced apoptosis in PC12 cells (Xiao et al., 2000). Recently, we have also reported that bis(7)-tacrine prevents glutamate-induced apoptosis in cerebellar granule neurons (CGNs) by blocking NMDAR (Li et al., 2005), and it attenuates NOS/NO-mediated neurotoxicity (Li et al., 2006) and β -amyloid-induced apoptosis in cortical neurons (Fu et al., 2006). It has also been found that although bis(7)-tacrine has a similar affinity and potency to memantine in blocking NMDAR, this dimer is much more potent than memantine in preventing glutamate-induced excitotoxicity in neurons (Li et al., 2005; Sonkusare et al., 2005).

In the present study, the molecular mechanisms underlying the more potent neuroprotection by bis(7)-tacrine are further examined in primary cultured neurons. We demonstrate that the substantial neuroprotection of bis(7)-tacrine may be concurrently mediated through direct and selective inhibition of nNOS as well as through moderate blockade of NMDAR, which plays a

MOL #29108

synergistic role in inhibiting endogenous NOS and then reducing NO generation. More importantly, at neuroprotective concentrations, bis(7)-tacrine has almost no interference with the basal activity of NOS in live neurons. The substrate kinetics of NOS inhibition and molecular simulation further indicate that bis(7)-tacrine selectively inhibits the neuronal subtype of NOS in a competitive manner.

MOL #29108

MATERIALS AND METHODS

Primary CGN Cultures. Rat CGNs were prepared from 8-day-old Sprague Dawley rats as described previously (Li et al., 2005). Briefly, neurons were seeded at a density of 2.0×10^6 cells/ml in basal modified Eagle's medium (Invitrogen, Carlsbad, CA, USA) containing 10% fetal bovine serum, 25 mM KCl, 2 mM glutamine, and penicillin (100 U/ml)/streptomycin (100 μ g/ml). Cytosine arabinoside (10 μ M) was added to the culture medium 24 h after plating to limit the growth of non-neuronal cells. With the use of this protocol, 95-99% of the cultured cells were granule neurons.

Measurement of Neurotoxicity. The percentage of surviving neurons was estimated by determining the activity of mitochondrial dehydrogenases with the 3(4,5-dimethylthiazol-2-yl)-2,5-diphenyltetrazolium bromide (MTT) assay (Li et al., 2005). The assay was performed according to the manufacturer's specifications (MTT Kit I, Roche Applied Science). Briefly, neurons were cultured in 96-well plates; 10 μ l of 5 mg/ml MTT labeling reagent was added to each well in 100 μ l of medium; and the plate was incubated for 4 h in a humidified incubator at 37 °C. After the incubation, 100 μ l of the solvating solution (0.01 N HCl in 10% SDS solution) was added to each well for 18 h. The absorbance of the samples was measured at a wavelength of 570 nm with 630 nm as a reference wavelength. Unless otherwise indicated, the extent of MTT conversion in the cells exposed to glutamate is expressed as a percentage of the control.

NO Release Detecting Assay. All electrochemical assays were performed with an Electrochemical Workstation in a 10 ml small, airtight beaker. For the sensors fabrication and NO measurements, the three-electrode system included an Au wire (Φ 0.5 mm) as the counter electrode, a modified Ag/AgCl wire (Φ 0.2 mm) as the reference electrode, and a chemically modified platinum microelectrode (Φ 50 μ m) with a modifier similar to that used in our previous

MOL #29108

report (Xue et al., 2000). In the electroanalytical experiments, a CHI660A Potentiostat was used with a preamplifier. The calibrated NO sensors were used for the following tests, which were conducted on the stage of an inverted stereomicroscope. The three-electrode system was bound together in order to ensure the immobile distance between each electrode. Under the stereomicroscope, the bound electrodes were positioned by about 10 μm close to the neurons. The data were qualitatively analyzed by differential pulse amperometry techniques.

Confocal Laser Scanning Microscopy. A confocal laser scanning microscope was used to evaluate relative changes in intracellular calcium concentrations ($[\text{Ca}^{2+}]_i$) by monitoring the Fluo-3 fluorescence after intracellular cleavage of a superfused Fluo-3 acetoxymethylester (5×10^{-6} M, with excitation at 488 nm and emission at > 510 nm) (Li et al., 2005). In brief, neurons were stained with 5×10^{-6} M Fluo-3 acetoxymethylester for 30 min in a 37 °C incubator and then washed three times with a balanced salt solution containing (in mM): NaCl 154, KCl 25, Na_2HPO_4 0.035, CaCl_2 2.3, NaHCO_3 3.6, glucose 5.6, HEPES 5, pH 7.4. The fluorescence images were analyzed using the MetaMorph software package (Universal Imaging Co., Downingtown, PA, USA). Data were obtained by evaluating the fluorescence (F) from selected areas within a cell, following subtraction of background fluorescence, and division by the fluorescence intensity before drug application (F_0), expressed as F/F_0 . Confocal images were taken and stored every 5-10 s. Bis(7)-tacrine was added to the balanced salt solution 30 min prior to the addition of glutamate.

Whole-Cell Electrophysiological Analysis. Cultures of hippocampal neurons on glial feeder layers were prepared from 15 to 17-day fetal mice for the whole-cell patch clamp analysis (Li et al., 2005). The hippocampi were dissected in Hank's Buffered Salt Solution containing 10 mM HEPES, DNase type I (Roche Applied Science), and 1 mM sodium pyruvate (pH 7.4); incubated

MOL #29108

in 0.25% trypsin (Invitrogen, Carlsbad, CA, USA) in Hank's Buffered Salt Solution at 37 °C for 15 min; washed three times in HBSS at room temperature; and triturated 30-40 times using a fire-polished Pasteur pipet. Neurons were plated on confluent layers of hippocampal glia in Minimum Essential Medium containing 10% heat-inactivated equine serum (HyClone, Logan, UT) and 1 mM sodium pyruvate. After 4 h, half of this medium was replaced with a maintenance medium consisting of Minimum Essential Medium, 1 mM sodium pyruvate, and N2 serum supplement (Invitrogen); this medium was subsequently given half-changes weekly. Neurons were cultured for two weeks prior to use in the experiments.

Whole-cell patch-clamp recording was carried out at room temperature using an EPC-7 patch clamp amplifier (Li et al., 2005; Strijbos et al., 1996). The membrane potential was held at -60 mV. Data were filtered at 2 kHz (8-pole Bessel) and acquired on a computer (5 kHz sampling frequency) during the experiments using a DigiData 1200A interface and pCLAMP software (Axon Instruments, Inc., Union City, CA, USA). Neurons were superfused at 1~2 ml min⁻¹ in an extracellular medium containing (in mM): NaCl, 150; KCl, 5; CaCl₂, 0.2; HEPES, 10; glucose, 10; tetrodotoxin, 0.0002; the pH was adjusted to 7.4 using NaOH and the osmolality to 340 mosmol kg⁻¹ using sucrose. Low Ca²⁺ was maintained to minimize NMDAR inactivation. The recording pipet solution contained (in mM): CsCl, 130; Mg₄ATP, 4; 1,2-bis(2-aminophenoxy) ethane-*N,N,N',N'*- tetraacetic acid, 10; HEPES, 10; pH was adjusted to 7.4 using CsOH and osmolality to 310 mosmol kg⁻¹ using sucrose. Solutions of agonists and drugs were prepared in extracellular media and were applied to neurons by gravity flow from a linear barrel array consisting of fused silica tubes (I.D. ~200 μm) connected to independent reservoirs; solutions were exchanged by shifting the pipette horizontally using a micromanipulator.

MOL #29108

Receptor-Ligand Binding Assay. The binding assay was performed and a synaptic plasma membrane was prepared from the cerebella of 15-day-old Sprague-Dawley rats by using discontinuous sucrose density gradients as described (Li et al., 2005). The receptor-ligand binding was performed in triplicate using 150~200 μg of the synaptic plasma membrane protein and 4 nM [^3H]MK-801 (American Radiolabeled Chemicals Inc; St.Louis, MO, USA) incubated with different concentrations of testing compounds; non-specific binding was determined by an excess of the cold MK-801. After collecting the samples on Whatman GF/B filters by rapid filtration with a MD-24 Sample Harvester, the filtrated tissue on the filters was soaked into scintillation cocktails overnight and measured in a scintillation counter (Wallac 1209 Rackbeta, Turku, Finland). Specific [^3H] ligand binding to receptors was determined by subtracting the non-specific count from the total, which is defined by 0.1 mM unlabeled MK-801. The K_i values are derived from the IC_{50} values by correcting for receptor occupancy by [^3H] ligand. The binding parameters were obtained with the ligand binding module in Sigmaplot 9.0 program.

NOS Activity Assays. For the NOS activity assay in neurons (Li et al., 2006), the activity of NOS was measured in CGNs by an assay kit (No. 482702 from Calbiochem, Darmstadt, Germany). The total levels of nitrate and nitrite were detected for indirectly reflecting NOS activity by following the kit's instructions. Ten μl supernatant of CGNs from 96-well plates exposed to 75 μM glutamate for 2 min was transferred into a fluorescent plate and incubated with 10 μl nitrate reductase and enzyme co-factors for 1 h at room temperature. Afterward, 10 μl 2,3-diaminonaphthalene was used as the substrate to react with the nitrite for 10 min. After quenching the reaction by adding 2.8 M NaOH, the fluorescent signal of the product, L(H)-naphthotriazole, was measured with the excitation of 365 nm and emission of 540 nm.

MOL #29108

The actual amount of nitrate was determined from the standard curves constructed by the nitrate standard provided.

In the *in vitro* NOS activity assay, purified recombinant human nNOS (Cat. No. 201-068-R100), endothelial NOS (eNOS) (Cat. No. 201-070-R100) and inducible NOS (iNOS) (Cat. No. 201-069-R100) were bought from Alexis Biochemicals (Lausen, Switzerland). NOS activity was determined by monitoring the conversion of L-[³H] arginine to [³H] citrulline following the kit's instructions (No. 482700 from Calbiochem, Darmstadt, Germany). The reaction mixture contained a final volume of 40 µl with 25 mM Tris-Cl at pH 7.4, 3 µM tetrahydrobiopterin, 1 µM FAD, 1 µM FMN, 1 mM NADPH, 0.6 mM CaCl₂, 0.1 µM calmodulin, 2.5 µg pure NOS enzyme, 5 µM L-[³H]-arginine (Amersham, City, IL, USA) and different concentrations of the tested reagents. The reaction mixture was incubated at 37°C for 30~45 min. The reaction was quenched by adding 400 µl stopping buffer (50 mM HEPES pH 5.5 and 5 mM EDTA) for nNOS and eNOS reactions, or by heating reactive tubes for iNOS. Unreacted L-[³H] arginine was then trapped by 100µl provided equilibrated resin in a spin cup followed by centrifugation for 1 min at 10,000 rpm. The filtrate was quantified by liquid scintillation counting.

Molecular Docking Technique. The crystal structures of nNOS, iNOS, and eNOS from the Protein Data Bank (Berman et al., 2000; Fedorov et al., 2004; Fischmann et al., 1999) were used in the docking studies. Ligands and water were removed from the crystal structures of the protein and hydrogen atoms were then added. The potential 3D structures of nNOS, iNOS and eNOS were assigned with Consistent Valence ForceField, which was encoded in the molecular modeling software Insight II (Accelrys, Inc., San Diego, CA, USA). The structure of bis(7)-tacrine was generated by Insight II. Automated molecular docking between all

MOL #29108

molecules was performed by using the advanced docking program, AutoDock 3.0.5, while the inhibitor-enzyme interactions were estimated by the Lamarckian Genetic Algorithm. A 3D grid with 52×52×52 points and a spacing of 0.375 Å was created by the AutoGrid algorithm (Morris et al., 1998) to evaluate the binding energies between proteins and ligands. At this stage, the protein was embedded in the 3D grid and a probe atom was placed at each grid point. The affinity and electrostatic potential grid were calculated for each type of atom in the ligand. The energetics of a particular inhibitor configuration was found by trilinear interpolation of affinity values and electrostatic interactions of the eight grid points surrounding each of the atoms of the ligand. A series of the docking parameters was set. The atom types as well as the generations and the number of runs for the LGA algorithm were edited and properly assigned according to the Amber force field requirements. The number of generations, energy evaluations, and docking runs were set to 370,000, 1,500,000, and 120, respectively. The docked complexes of the ligand-enzyme were selected according to the interacting energy combined with the geometrical matching quality.

Data Analysis and Statistics. Data are expressed as mean ± SEM, and statistical significance was determined by analysis of variance (ANOVA) with Dunnett's test. Differences were accepted as significant at $p < 0.05$ or less.

MOL #29108

RESULTS

NO Mediates Glutamate-Induced Excitotoxicity in Neurons. At 8 days *in vitro* (DIV), CGNs were exposed to glutamate at concentrations from 0 to 150 μM . The cell viability was detected by MTT assay at 24 h after the glutamate challenge; and the NO release was measured by electrochemical methods from 10 min before to 30 min after the glutamate challenge. As shown in Fig. 1A, glutamate caused NO release and cell death in a concentration-dependent manner. CGNs were then pretreated with 10 to 200 μM of L-NMMA for 2 h and exposed to 75 μM glutamate for 24 h. We found that L-NMMA inhibited the release of NO and the cell death caused by glutamate in a concentration-dependent manner (Fig. 1B and 1C). Furthermore, we also observed earlier that both L-NMMA at 100 μM and carboxy-PTIO (a NO scavenger) at 10 μM significantly prevent glutamate-induced excitotoxicity in primary cultured cortical neurons (Li et al., 2006).

Bis(7)-tacrine Prevents Glutamate-Induced Excitotoxicity and NO Release More Potently than Do Memantine and L-NMMA. As shown in Fig. 1B, CGNs were pretreated with bis(7)-tacrine (0.1 nM to 1 μM), MK-801 (0.1 nM to 1 μM), memantine (10 nM to 50 μM) and L-NMMA (10 μM to 200 μM) for 2 h and exposed to 75 μM glutamate for 24 h. It was found that bis(7)-tacrine, MK-801, memantine and L-NMMA prevented glutamate-induced cell death in a concentration-dependent manner with $\text{EC}_{50\text{s}}$ of 0.024, 0.023, 2.0 and 81.7 μM , respectively. Furthermore, we also found that the selective nNOS inhibitors 7-NI and L-thiocitrulline prevented glutamate-induced cell death with $\text{EC}_{50\text{s}}$ of 14.7 and 5.9 μM , respectively. We also compared the effects of MK-801, memantine and L-NMMA, and bis(7)-tacrine on the NO release triggered by glutamate using electrochemical methods. As shown in Fig. 1C,

MOL #29108

bis(7)-tacrine, MK-801, memantine and L-NMMA reduced the NO release triggered by 75 μ M glutamate in a concentration-dependent manner with IC_{50} s of 0.052, 0.012, 6.8 and 54.6 μ M, respectively. Similar to L-NMMA, bis(7)-tacrine had higher efficacy than MK-801 and memantine in reducing NO release triggered by glutamate (Fig. 1C).

Bis(7)-tacrine Prevents the Excitotoxicity and NO Release Caused by Glutamate in a Time-Dependent Manner. Compared with 50 μ M L-NMMA/5 μ M memantine/0.1 μ M MK-801, at various pretreatment and concurrent durations, 0.1 μ M bis(7)-tacrine significantly prevented the death of CGNs induced by glutamate; and still showed significant neuroprotective effects even when added at 1 h after the glutamate insult (*strip bar* in Fig. 2A), but the potency of its neuroprotective effects significantly decreased with gradually reduced treatment times ($p < 0.01$ between different pre-, concurrent or post-treatment times, ANOVA and Dunnett's test) and completely had no effect when added at 2 h after the glutamate insult. The time course fashion of bis(7)-tacrine, similar to that of L-NMMA, was different from that of MK-801 and memantine in preventing the excitotoxicity caused by glutamate ($p > 0.05$ between different pretreatment times, ANOVA and Dunnett's test); and we also found that MK-801 and memantine lost their neuroprotective effects when added 1 h after the glutamate challenge (*strip bar* in Fig. 2A). Similar to their neuroprotection abilities, the effects of bis(7)-tacrine and L-NMMA at various pre- and concurrent treatment times ($p < 0.01$ between different pre- or concurrent treatment times, ANOVA and Dunnett's test) were different from those of MK-801 and memantine ($p > 0.05$ between different pretreatment times, ANOVA and Dunnett's test) in reducing the NO release triggered by 75 μ M glutamate (Fig. 2B).

Bis(7)-tacrine Blocks NMDAR Moderately. In primary cultured hippocampus neurons at 12

MOL #29108

DIV, whole cell currents were recorded at 100 μM NMDA alone or with the tested drugs. It was found that bis(7)-tacrine, similar to memantine but weaker than MK-801, inhibited NMDA-evoked inward currents (*left column* of Table 1; Supplemental Data). According to the ligand-receptor binding assay, the affinity of bis(7)-tacrine consistently competed with [^3H]MK-801 in rat cerebellar cortical membranes similar to that of memantine but much weaker than that of MK-801 (*middle column* of Table 1). Furthermore, in CGNs at 8 DIV, glutamate at 50 μM increased intracellular Ca^{2+} by 2.5-times the basal level; and at 1 μM of the tested drugs, bis(7)-tacrine, close to memantine but weaker than MK-801, significantly reduced the increase of intracellular Ca^{2+} triggered by glutamate (*right column* of Table 1). However, NOS inhibitors L-NMMA and 7-NI at neuroprotective concentrations failed to inhibit the NMDA-evoked currents in the neurons, failed to compete with [^3H]MK-801 in rat cerebellar cortical membranes, and failed to reduce the increase of intracellular Ca^{2+} triggered by glutamate in CGNs (Table 1), which indicated that L-NMMA and 7-NI did not directly interfere with the NMDAR.

Bis(7)-tacrine Inhibits NOS *in Vivo* and *in Vitro*. In the NOS activity assays in CGNs, when each of tested drugs was set at 1 μM , we found that bis(7)-tacrine, similar to L-NMMA, slightly inhibited the basal activity of endogenous NOS in CGNs although its potency was higher than the potency of memantine (*left panel* of Table 2). However, in inhibiting the activity of NOS activated by 75 μM glutamate in CGNs, based on the IC_{50} values, bis(7)-tacrine was approximately 1453 and 250 times more potent than L-NMMA and memantine, respectively (*right panel* of Table 2). In an *in vitro* NOS activity assay, bis(7)-tacrine was further found to be both direct and more selective in inhibiting recombinant human nNOS over iNOS rather than the eNOS. However, MK-801 and memantine did not inhibit any of the isozymes even at 1

MOL #29108

mM. Furthermore, bis(7)-tacrine possessed higher selectivity to nNOS/iNOS over eNOS than 7-NI and L-NMMA *in vitro* (Table 3).

Bis(7)-tacrine Inhibits nNOS and iNOS in a Competitive Manner. To investigate the patterns of bis(7)-tacrine in nNOS and iNOS inhibition, 1 and 3 μM bis(7)-tacrine were added to the reaction system of nNOS or iNOS reaction systems with L-arginine at concentrations from 5 to 40 μM , respectively. As shown in Fig. 3A, in the Lineweaver-Burk plots, the inhibitory straight-lines of bis(7)-tacrine converged on the Y axis ($V_{\text{max}} = 0.041 \mu\text{mol}/\text{mg}\cdot\text{min}$), indicating that bis(7)-tacrine inhibited nNOS by competing with L-arginine. Compared with L-NMMA ($K_i = 3.7 \mu\text{M}$), bis(7)-tacrine inhibited nNOS with K_i at 1.7 μM ($K_m = 6.3 \mu\text{M}$ of L-arginine alone) (Fig. 4B). On the other hand, bis(7)-tacrine also competitively inhibited iNOS with L-arginine; and compared with L-NMMA ($K_i = 9.1 \mu\text{M}$), bis(7)-tacrine inhibited iNOS with K_i at 5.8 μM ($K_m = 8.1 \mu\text{M}$ of L-arginine alone).

Molecular Docking Simulation of the Interaction between Bis(7)-tacrine and NOS

Isozymes. In order to gain further insight into the interaction mechanisms between bis(7)-tacrine and three NOS isoforms, computational docking was performed to dock bis(7)-tacrine separately to nNOS, iNOS and eNOS. The estimated free energy of bis(7)-tacrine binding to nNOS had the lowest value (-14.93 kcal/mol) when compared with those of bis(7)-tacrine binding to iNOS (-14.17 kcal/mol) and eNOS (-13.35 kcal/mol). In the bis(7)-tacrine-nNOS complex, hydrogen bonds were formed at the tacrine moiety with Glu592 and the heme at the bottom of the pocket (Fig. 4A-a); and in the bis(7)-tacrine-iNOS complex, the same type of bonds were formed between the tacrine moiety and the amino acids Glu371 (at the bottom of the pocket), Glu488 and Asn348 (near the top of the pocket) (Fig. 4A-b); a

MOL #29108

hydrogen bond was only formed between Glu361 and the tacrine moiety in the bis(7)-tacrine-eNOS complex (Fig. 4A-c). Furthermore, there were two characteristics of the interactions between bis(7)-tacrine and NOS isoforms: a glutamate (Glu592 of nNOS, Glu371 of iNOS, and Glu361 of eNOS) located at the pocket bottom formed a hydrogen bond with the nitrogen atom of one tacrine moiety of bis(7)-tacrine (Fig. 4Ba-c); and bis(7)-tacrine formed hydrophobic interactions with nNOS and iNOS at both the bottom and top of the pocket (Fig. 4Aa-b).

MOL #29108

DISCUSSION

We have reported that bis(7)-tacrine prevents glutamate-induced neuronal apoptosis in CGNs (Li et al., 2005). In the current study, the model of glutamate-induced excitotoxicity in CGNs was used to investigate further the precise mechanisms underlying the superior neuroprotective activities of bis(7)-tacrine. In CGNs, there is a correlation between the excitotoxicity and NO release caused by glutamate (Fig. 1A); and the NOS inhibitor L-NMMA significantly reduced the NO release and the cell death induced by glutamate (Fig. 1B and 1C). Furthermore, both selective nNOS inhibitors (7-NI and L-thiocitrulline) and a NO scavenger [2-(4-carboxyphenyl)-4,4,5,5-tetra-methyl-imidazoline-1-oxyl-3-oxide] significantly prevented glutamate-induced neurotoxicity (Li et al., 2006). Together, these results suggest that NO mediates glutamate-induced excitotoxicity. Since bis(7)-tacrine can significantly reduce glutamate-induced excitotoxicity (Li et al., 2005), we investigated how bis(7)-tacrine affected glutamate-induced NO generation. As shown in Figs. 1B and C, similar to MK-801, bis(7)-tacrine was approximately 80 and 3400 times more potent in reducing the excitotoxicity and 130 and 1050 times potent in inhibiting the NO release than were memantine and L-NMMA, respectively. These results indicate that there is a correlation between neuroprotection and the inhibitory ability of NO formation by bis(7)-tacrine.

How did bis(7)-tacrine inhibit the NO release induced by glutamate at such high potency? Endogenous NO is produced only by NOS when L-arginine is converted into L-citrulline (Blaise et al., 2005; Fedorov et al., 2004). Therefore, the reduction of NO may be caused by either inhibiting NOS or scavenging NO. Bis(7)-tacrine fails to inhibit the cell death and the NO release induced by a NO donor sodium nitroprusside (Li et al., 2006), indicating that the inhibition of NO generated by NOS may contribute to the neuroprotection of bis(7)-tacrine

MOL #29108

instead of scavenging NO. Excessive glutamate may overactivate NOS through overloading intracellular Ca^{2+} and/or altering the conformation of the postsynaptic density protein-95 – NMDAR coupling protein; and the blockade of NMDAR or the interference of this coupling protein may inhibit the activation of NOS caused by glutamate (Aarts et al., 2002; Sattler et al., 1999). However, bis(7)-tacrine failed to interfere with their interaction (data not shown), suggesting that the NO inhibition is likely to be via an NMDAR blockade. Our results indeed suggested that bis(7)-tacrine, similarly to memantine but much more weakly than MK-801, blocks NMDAR at the MK-801 site and then reduces glutamate-triggered increase of intracellular Ca^{2+} (Table 1), which may contribute to the inhibition of NO production via indirectly inhibiting NOS. However, how do we explain the discrepancy between the moderate blockade of NMDAR and the high neuroprotection potency by bis(7)-tacrine?

Bis(7)-tacrine, as well as L-NMMA, significantly inhibits NO-mediated neuronal cell death caused by glutamate and L-arginine and in cortical neurons (Li et al., 2006), while MK-801 cannot prevent neuronal cell death induced by L-arginine (Yamauchi et al., 1998). Under various different treatment durations, the time-dependent potency of bis(7)-tacrine, similar to that of L-NMMA, was different from that of MK-801 and memantine in reducing cell death and NO release. Moreover, bis(7)-tacrine and L-NMMA still possessed significant neuroprotective effects even when added 1 h after glutamate challenge (Fig. 2). Together, these findings suggest that besides blocking NMDAR, bis(7)-tacrine may have intracellular targets for NOS inhibition. Therefore, we hypothesized that bis(7)-tacrine might directly inhibit the activity of NOS in this study. In live neurons, bis(7)-tacrine showed significant neuroprotection effects at low concentrations (such as 1 nM in Fig. 1B), which is matched with its high inhibitory potency for glutamate-induced NO release and NOS activation. *In vitro*, bis(7)-tacrine directly inhibited the activity of purified NOS with higher selectivity towards nNOS and iNOS (Table 3).

MOL #29108

Furthermore, bis(7)-tacrine did not alter V_{max} , but increased the observed K_m (Fig. 3A); and the observed K_m and corresponding concentration of bis(7)-tacrine had a linear relationship (Fig. 3B). Our results suggest that bis(7)-tacrine directly inhibits nNOS and iNOS in a competitive way with L-arginine.

By using the docking simulation technique, we investigated the molecular interaction mechanisms between bis(7)-tacrine and three NOS isozymes. In the bis(7)-tacrine-nNOS complex, the tacrine moiety closely contacted with Tyr706 (Fig. 4A-a). The hydrophobic interaction between bis(7)-tacrine and Tyr706 facilitated a long inhibition with nNOS. Since bis(7)-tacrine is also a bivalent inhibitor of AChE (Pang et al., 1996), aromatic residues such as Trp279 and Tyr70 that are located at the peripheral site of the AChE gorge can also form hydrophobic interactions with any bivalent AChE inhibitors such as donepezil, which control the bivalent inhibitors entering or leaving the gorge (Kryger et al., 1999; Niu et al., 2005). Therefore, we conclude that the aromatic residue of Tyr706 also plays an important role in controlling the bis(7)-tacrine binding in nNOS. In the bis(7)-tacrine-iNOS complex, although bis(7)-tacrine formed hydrogen bonds with Asn348 and Glu488, the affinity of bis(7)-tacrine to iNOS was actually lower than that with nNOS, which may be due to the further distance between the bis(7)-tacrine and Y485 (Fig. 4A-b). In the bis(7)-tacrine-eNOS complex, bis(7)-tacrine only formed hydrophobic interactions with Trp447 at the top of the pocket (Fig. 4A-c), which therefore causes the lowest affinity of bis(7)-tacrine to eNOS among the three NOS isoforms.

NO, as well as glutamate, is an important bio-regulatory molecule in various organs for daily activities of cells. It is only at elevated concentrations that NO and glutamate are involved in cytotoxic events (Aarts et al., 2002; Drummond et al., 2005). Therefore, it is of great significance to find drugs that inhibit the overactivation of NMDAR and NOS instead of

MOL #29108

interfering with NO and glutamate's normal physiological functions. Moderate affinity antagonists of NMDAR, such as memantine, actually have high success in the treatment of numerous central nervous system disorders because drugs with this property may prevent glutamate excitotoxicity without producing undesirable side effects within the therapeutic dosages, while high affinity antagonists such as MK-801 may produce severe adverse effects (Danysz and Parsons, 2003; Li et al., 2005). Very interestingly, bis(7)-tacrine has a moderate affinity to NMDAR (Table 1). Furthermore, bis(7)-tacrine has been shown to cross the brain-blood barrier easily (Wang et al., 1999) with no significant side effect at the proposed therapeutic dosages (Liu et al., 2000). On the other hand, bis(7)-tacrine at 1 μM nearly completely prevents glutamate-induced cell death while only slightly inhibiting the basal activity of NOS in CGNs (Table 2), indicating that, at effective concentrations, this compound may not interfere with the normal physiological functions of NO. Even though L-NMMA at 1 μM also slightly inhibited NOS basal activity, it exhibited significant neuroprotective effects only at high concentrations (more than 50 μM in Fig. 1B), which is matched with its relatively lower ability in reducing the glutamate-induced NOS activation (Table 2). It can be rationally proposed that L-NMMA at effective neuroprotective concentrations may also strongly inhibit the activity of physiological NOS and the normal functioning of NO. Furthermore, bis(7)-tacrine possesses higher selectivity towards nNOS and iNOS than eNOS *in vitro*. In addition, the activation of iNOS is independent of intracellular Ca^{2+} increases triggered by glutamate (Alderton et al., 2001; Strub et al., 2006). Therefore, bis(7)-tacrine at neuroprotective concentrations may inhibit the activity of nNOS overactivated by glutamate without interfering with eNOS and iNOS. Very encouragingly, synergistic neuroprotective effects have been shown by combining an NMDA receptor antagonist with nitric oxide

MOL #29108

inhibitors in the treatment of cerebral ischemia (Hicks et al., 1999). In our system, we found that 0.1 μM memantine combined with 10 μM L-NMMA or with 10 μM 7-NI were much more potent than each chemical alone in reducing the excitotoxicity caused by glutamate (Fig. 5A), suggesting that the concurrent blockage of NMDAR and NOS may be synergistically neuroprotective against the excitotoxicity.

In summary, bis(7)-tacrine prevents glutamate-induced excitotoxicity by the reduction of excessive NO release through inhibiting nNOS in both direct (i.e., inhibition of nNOS) and indirect (i.e., moderately blocking NMDAR, which reduces the influx of Ca^{2+} and inhibits NOS activation) mechanisms, which are a synergistically neuroprotective (Fig. 5B). Although further studies are needed to rule out other possible targets, here we can conclude that at least the concurrent blockade of NMDAR and neuronal NOS is involved in the mechanisms underlying neuroprotection by bis(7)-tacrine. This conclusion may explain why bis(7)-tacrine has higher potency than memantine or L-NMMA in glutamate-induced excitotoxicity although it possesses similar potency to block NMDA receptors as does memantine, or to inhibit nNOS as does L-NMMA *in vitro*. Our findings here strongly suggest that the novel AChE inhibitor bis(7)-tarine is also a moderate NMDAR antagonist and a selective nNOS inhibitor. Given burgeoning and increasing evidence suggesting that multi-functional compounds might provide greater therapeutic efficacy for neurodegenerative diseases by concurrently targeting different sites in the brain (Youdim et al., 2005), these and our previously published results lead us to conjecture that the multi-potencies of bis(7)-tacrine may synergistically contribute to reducing the effects of various neurodegenerative disorders, which may offer a novel direction for rational development of new agents for the prevention and treatment of neurodegenerative diseases.

MOL #29108

REFERENCES

- Aarts M, Liu Y, Liu L, Besshoh S, Arundine M, Gurd JW, Wang YT, Salter MW, and Tymianski M (2002) Treatment of ischemic brain damage by perturbing NMDA receptor- PSD-95 protein interactions. *Science* **298**: 846-850.
- Alderton WK, Cooper CE, and Knowles RG (2001) Nitric oxide synthases: structure, function and inhibition. *Biochem. J.* **357**: 593-615.
- Berman HM, Westbrook J, Feng Z, Gilliland G and Bhat TN (2000) The Protein Data Bank. *Nucleic. Acids. Res.* **28**: 235-242.
- Blaise GA, Gauvin D, Gangal M, and Authier S (2005) Nitric oxide, cell signaling and cell death. *Toxicology* **208**: 177-192.
- Danysz W and Parsons CG (2003) the NMDA receptor antagonist memantine as symptomatological and neuroprotective treatment for Alzheimer's disease: preclinical evidence. *Int. J. Geriatr. Psychiatry* **18**, S23-32.
- Drummond JC, McKay LD, Cole DJ and Patel PM (2005) The role of nitric oxide synthase inhibition in the adverse effects of etomidate in the setting of focal cerebral ischemia in rats. *Anesth. Analg.* **100**: 841-846.
- Fedorov R, Vasani R, Ghosh DK and Schlichting I (2004) Structures of nitric oxide synthase isoforms complexed with the inhibitor AR-R17477 suggest a rational basis for specificity and inhibitor design. *Proc. Natl. Acad. Sci. USA* **101**: 5892-5897.
- Fischmann TO, Hruza A, Xiao DN, Fossetta JD, Lunn CA, Dolphin E, Prongay AJ, Reichert P, Lundell DJ, Narula SK and Weber PC (1999) Structural characterization of nitric oxide synthase isoforms reveals striking active-site conservation. *Nat. Struct. Biol.* **6**: 233-242.
- Frantz S. (2005) Drug discovery: playing dirty. *Nature* **437**, 942-943.
- Fu H, Li W, Lao Y, Luo J, Lee NT, Kan KK, Tsang HW, Tsim KW, Pang Y, Li Z, Chang DC, Li M and Han Y (2006) Bis(7)-tacrine attenuates beta amyloid-induced neuronal apoptosis by regulating L-type calcium channels. *J. Neurochem.* **98**, 1400-1410.
- Grunewald T and Beal MF (1999) NOS knockouts and neuroprotection. *Nat. Med.* **5**: 1354-1355.

MOL #29108

- Hicks CA, Ward MA, Swettenham JB and O'Neill MJ. (1999) Synergistic neuroprotective effects by combining an NMDA or AMPA receptor antagonist with nitric oxide synthase inhibitors in global cerebral ischaemia. *Eur. J. Pharmacol.* **381**: 113-119.
- Kryger G, Silman I and Sussman JL (1999) Structure of acetylcholinesterase complexed with E2020 (Aricept); implications for the design of new anti-Alzheimer drugs. *Structure. Fold. Des.* **7**: 297-307.
- Li W, Lee NT, Fu H, Kan KK, Pang Y, Li M, Tsim KW and Han Y (2006) Neuroprotection via inhibition of nitric oxide synthase by bis(7)-tacrine. *Neuroreport* **17**: 471-475.
- Li W, Pi R, Chan HH, Fu H, Lee NT, Tsang HW, Pu Y, Chang DC, Li C, Luo J, Xiong K, Li Z, Xue H, Carlier PR, Pang Y, Tsim KW, Li M, and Han Y (2005) Novel dimeric acetylcholinesterase inhibitor bis7-tacrine, but not donepezil, prevents glutamate-induced neuronal apoptosis by blocking N-methyl-D-aspartate receptors. *J. Biol Chem.* **280**: 18179-88.
- Liu J, Ho W, Lee NT, Carlier PR, Pang Y, and Han Y (2000) Bis(7)-tacrine, a novel acetylcholinesterase inhibitor, reverses AF64A-induced deficits in navigational memory in rats. *Neurosci. Lett.* **282**: 165-168.
- Lipton SA (2004) Paradigm shift in NMDA receptor antagonist drug development: molecular mechanism of uncompetitive inhibition by memantine in the treatment of Alzheimer's disease and other neurologic disorders. *J Alzheimers Dis.* **6**, S61-74.
- Mattson MP (2004) Pathways towards and away from Alzheimer's disease. *Nature* **430**, 631-639.
- Morris GM, Goodsell DS, Halliday RS, Huey R, Hart WE, Belew RK and Olson AJ (1998) Automated docking using a Lamarckian genetic algorithm and an empirical binding free energy function. *J. Comput. Chem.* **19**: 1639-1662.
- Niu CY, Xu YC, Xu Y, Luo XM, Duan WH, Silman I, Sussman JL, Zhu WL, Chen KX, Shen JH and Jiang HL (2005) Dynamic mechanism of E2020 binding to acetylcholinesterase: a steered molecular dynamics simulation. *J. Phys. Chem. B.* **109**: 23730-23738.
- Pang YP, Quiram P, Jelacic T, Hong F, and Brimijoin S (1996) Highly potent, selective, and low cost bis-tetrahydroaminacrine inhibitors of acetylcholinesterase. Steps toward novel drugs for treating Alzheimer's disease. *J. Biol. Chem.* **271**: 23646-23649.

MOL #29108

- Sattler R, Xiong Z, Lu WY, Hafner M, MacDonald JF and Tymianski M (1999) Specific coupling of NMDA receptor activation to nitric oxide neurotoxicity by PSD-95 protein. *Science* **284**, 1845-1848.
- Sonkusare SK, Kaul CL, and Ramarao P (2005) Dementia of Alzheimer's disease and other neurodegenerative disorders--memantine, a new hope. *Pharmacol. Res.* **51**: 1-17.
- Strijbos PJ, Leach MJ, and Garthwaite J (1996) Vicious cycle involving Na⁺ channels, glutamate release, and NMDA receptors mediates delayed neurodegeneration through nitric oxide formation. *J. Neurosci.* **16**: 5004-5013.
- Strub A, Ulrich WR, Hesslinger C, Eltze M, Fuchss T, Strassner J, Strand S, Lehner MD and Boer R. (2006) The novel imidazopyridine 2-[2-(4-methoxy-pyridin-2-yl)-ethyl]-3H-imidazo [4,5-b] pyridine (BYK191023) is a highly selective inhibitor of the inducible nitric-oxide synthase. *Mol. Pharmacol.* **69**: 328-337.
- Van der Schyf CJ, Geldenhuys WJ and Youdim MB (2006) Multifunctional drugs with different CNS targets for neuropsychiatric disorders. *J. Neurochem.* **99**, 1033-1048.
- Wang H, Carlier PR, Ho WL, Wu DC, Lee NT, Li CP, Pang YP, and Han YF (1999) Effects of bis(7)-tacrine, a novel anti-Alzheimer's agent, on rat brain AChE. *Neuroreport* **10**, 789-793.
- Willmot M, Gibson C, Gray L, Murphy S and Bath P (2005) Nitric oxide synthase inhibitors in experimental ischemic stroke and their effects on infarct size and cerebral blood flow: a systematic review. *Free Radic Biol Med.* **39**, 412-25.
- Wu DC, Xiao XQ, Ng AK, Chen PM, Chung W, Lee NT, Carlier PR, Pang YP, Yu AC, and Han YF (2000) Protection against ischemic injury in primary cultured mouse astrocytes by bis(7)-tacrine, a novel acetylcholinesterase inhibitor. *Neurosci. Lett.* **288**, 95-98.
- Xiao XQ, Lee NT, Carlier PR, Pang Y, and Han YF (2000) Bis(7)-tacrine, a promising anti-Alzheimer's agent, reduces hydrogen peroxide-induced injury in rat pheochromocytoma cells: comparison with tacrine. *Neurosci. Lett.* **290**, 197-200.
- Xue J, Ying X, Chen J, Xian Y and Jin L (2000) Amperometric ultramicrosensors for peroxynitrite detection and its application toward single myocardial cells. *Anal Chem.* **72**: 5313-5321.

MOL #29108

Yamauchi M, Omote K, and Ninomiya T (1998) Direct evidence for the role of nitric oxide on the glutamate-induced neuronal death in cultured cortical neurons. *Brain Res.* **780**: 253-259.

Youdim MB and Buccafusco JJ (2005) Multi-functional drugs for various CNS targets in the treatment of neurodegenerative disorders. *Trends Pharmacol Sci* **26**, 27-35.

Yuan J and Yankner BA (2000) Apoptosis in the nervous system. *Nature* **407**: 802-809.

Zhang HY (2005) One-compound-multiple-targets strategy to combat Alzheimer's disease. *FEBS Lett* **579**, 5260-5264.

MOL #29108

FOOTNOTES

This work was supported by grants from the Research Grants Council of Hong Kong (HKUST 6120/02M, 6133/03M, 6140/02M and 6441/06M; 643/99; AoE/B15/01; P_10/01); the National Science Foundation of China (30370450, 30170299 and 30570562) and the CPD Foundation (20060390210). We sincerely thank Professor Donald C. Chang for kindly providing the confocal laser scanning microscopy for the intracellular calcium assay and Dr. Virginia Anne Unkefer for carefully editing and proofreading our manuscript.

Address Reprint Requests to:

Dr. Yifan Han, Associate Professor. Department of Biochemistry, Hong Kong University of Science and Technology, Clear Water Bay, Kowloon, Hong Kong SAR, China.

Tel.: 852-23587293; Fax: 852-23581552; E-mail: bcyfhan@ust.hk

MOL #29108

FIGURE LEGENDS

Fig. 1. Bis(7)-tacrine prevents glutamate-induced excitotoxicity and NO release more potently than do memantine and L-NMMA. **A.** Correlation between glutamate-induced excitotoxicity and NO release. For detecting the excitotoxicity of glutamate, at 8 DIV, CGNs were exposed to glutamate at the concentrations indicated. At 24 h after the challenges, the cell viability was measured by MTT assay. All of the data, expressed as the rates of cell death (100 – the percentage of Control), are the means \pm S.E.M. of three separate experiments; *, $p < 0.05$; **, $p < 0.01$ versus control (ANOVA and Dunnett's test). For detecting the NO release by glutamate, CGNs were exposed to glutamate at the concentrations indicated and NO concentrations were assayed by the electrochemical method simultaneously. The data were calculated as described in the Materials and Methods section; +, $p < 0.05$; ++, $p < 0.01$ versus control (ANOVA and Dunnett's test). **B.** Bis(7)-tacrine prevents glutamate-induced excitotoxicity more potently than do memantine and L-NMMA. At 8 DIV, CGNs were pretreated with bis(7)-tacrine (0.1 nM to 1 μ M)/MK-801 (0.1 nM to 1 μ M)/memantine (10 nM to 50 μ M)/L-NMMA (10 to 200 μ M) for 2 h before the addition of glutamate (75 μ M). The cell viability was measured at 24 h after glutamate challenge. All of the data, expressed as percentages of the corresponding control, are the means \pm S.E.M. of three separate experiments. **C.** Bis(7)-tacrine prevents glutamate-induced NO release more potently than do memantine and L-NMMA. At 8 DIV, CGNs were pretreated with bis(7)-tacrine/MK-801/memantine/L-NMMA at the above indicated concentrations for 2 h before the addition of glutamate (75 μ M). NO concentrations were measured by the electrochemical method.

Fig. 2. The time-dependent potency profile of bis(7)-tacrine preventing the excitotoxicity and NO release caused by glutamate. **A.** Bis(7)-tacrine prevents the excitotoxicity in a

MOL #29108

time-dependent manner. CGNs were exposed to 0.1 μM bis(7)-tacrine/0.1 μM MK-801/5 μM memantine/100 μM L-NMMA 24, 12 and 2 h before glutamate at 75 μM (-24, -12 and -2 h), at the same time as glutamate (0), or 1 and 2 h after glutamate (1 and 2 h). At 24 h after the glutamate challenge, the cell viability was measured by MTT assay. All of the data, expressed as percentages of the corresponding control, are the means \pm S.E.M. of three separate experiments. **B.** Bis(7)-tacrine prevents NO release in a time-dependent manner. CGNs were exposed to 0.1 μM bis(7)-tacrine/0.1 μM MK-801/5 μM memantine/100 μM L-NMMA 24, 12 or 2 h before glutamate at 75 μM (-24, -12 or -2 h) or at the same time as glutamate (0). The NO release was detected and the data were calculated as described in the Materials and Methods section.

Fig. 3. Selective inhibition of nNOS by bis(7)-tacrine in a competitive manner. **A.** Pattern analysis of nNOS inhibition with L-arginine by bis(7)-tacrine. Recombinant nNOS (2.5 μg) was assayed in either the presence (1 μM or 3 μM) or the absence of bis(7)-tacrine under the conditions with 5 to 40 μM L-[^3H] arginine. The plots of $1/V$ versus $1/[S]$ were fitted by a Lineweaver-Burk straight-line with an intercept of $1/V_{\text{max}}$ and a slope of K_m/V_{max} . The data are expressed as the means from three independent experiments. **B.** The K_i value of bis(7)-tacrine to inhibit nNOS. The plot of the observed K_m values from **A** versus concentrations of bis(7)-tacrine was drawn by the linear fit.

Fig. 4. Molecular docking simulation of selective interactions between bis(7)-tacrine and nNOS. **A.** Schematic representation of hydrogen bonds and hydrophobic interactions between bis(7)-tacrine and nNOS (a), iNOS (b) and eNOS (c). The dashed lines represent the hydrogen bonds and spiked residues form the hydrophobic interactions with bis(7)-tacrine. This picture

MOL #29108

was made with the LIGPLOT program. **B.** The patterns of selective interactions between bis(7)-tacrine and nNOS (a), iNOS (b) and eNOS (c). The figures were prepared using the PYMOL program.

Fig. 5. Concurrent blockage of NMDAR and nNOS shows the proposed dual mechanism of synergistic neuroprotection against glutamate. **A.** Synergistic protection against glutamate-induced excitotoxicity by combination of memantine and L-NMMA or 7-NI. At 8 DIV, CGNs were exposed to 0.1 μ M memantine/10 μ M L-NMMA/10 μ M 7-NI/(0.1 μ M memantine + 10 μ M L-NMMA)/(0.1 μ M memantine + 10 μ M 7-NI) for 2 h before glutamate at 75 μ M. At 24 h after the glutamate challenge, the cell viability was measured by MTT assay. All of the data, expressed as percentages of the corresponding control, are the means \pm S.E.M. of three separate experiments; *, $p < 0.05$ versus glutamate alone group; ##, $p < 0.01$ versus memantine, L-NMMA or 7-NI alone (ANOVA and Dunnett's test). **B.** The proposed dual mechanism of synergistic neuroprotection against glutamate by bis(7)-tacrine. When neurons are exposed to glutamate at toxic concentrations, excessive NO mediates NMDAR downstream signaling pathways that trigger excitotoxicity. Bis(7)-tacrine concurrently blocks NMDAR and inhibits nNOS, thereby synergistically providing substantial neuroprotection.

MOL #29108

TABLE 1

Bis(7)-tacrine moderately blocks NMDA receptors

	NMDA current*	[³ H] MK-801 binding [#]	Ca ²⁺ influx [¶]
	IC ₅₀ (μM)	K _i (μM)	F / F ₀
Control			2.5 ± 0.27
Bis(7)-tacrine	2.5 ± 0.53	0.7 ± 0.045	1.7 ± 0.14
Memantine	3.7 ± 0.69	0.8 ± 0.055	1.9 ± 0.17
MK-801	0.05 ± 0.017	0.04 ± 0.024	1.1 ± 0.13
L-NMMA		-----ND [§] -----	
7-NI		-----ND-----	

*Whole cell currents were recorded from NMDA (100 μM) alone or NMDA with bis(7)-tacrine/memantine/MK-801/L-NMMA/7-NI at the serial concentrations on primary cultured hippocampal neurons as described under the Materials and Methods section. The IC₅₀ values of these chemicals for inhibiting NMDA-evoked currents were calculated by Sigmaplot 9.0 according to the corresponding concentration-response curves. [#]The membrane proteins from rat cerebellar cortex were incubated with [³H]MK-801 (4 nM) as described in the Materials and Methods section. The K_i values were calculated from the corresponding IC₅₀ values, which were measured from data obtained using at least eight concentrations of each chemical (in duplicates), based on the Cheng-Prusoff equation, namely $K_i = IC_{50} / (1 + [ligand] / K_d)$. [¶]The intracellular calcium was detected by Confocal microscopy with Flou-3 dye. The data are expressed as F / F₀ (F, the fluorescence value after exposure to 50 μM glutamate 10 min with the indicated chemical; F₀, the fluorescence value just before exposure to glutamate; n = 30 for each group). [§]ND means ‘not detectable’, which indicate that the corresponding chemical have no effect on the tested items.

MOL #29108

TABLE 2

Differential inhibition of basal and overactivated nNOS by bis(7)-tacrine

Drug	Basal NOS (without glutamate)	Activated NOS (with glutamate)
	*Relative Inhibitory Potency at 1 μ M	#IC ₅₀ , μ M
Bis(7)-tacrine	4.5 \pm 0.36%	0.03 \pm 0.0061
L-NMMA	3.7 \pm 0.45%	43.6 \pm 5.73
Memantine	0.8 \pm 0.29%	7.5 \pm 0.96

The activity of NOS and its inhibition by different chemicals were measured in CGNs by the NOS assay kit as described in the Materials and Methods section. *Relative Inhibitory Potency was expressed as $[1 - (\text{NOS activity of group with the drug at } 1 \mu\text{M over that of control group})] \times 100\%$. #IC₅₀ value of each chemical to inhibit endogenous NOS in CGNs treated with glutamate at 75 μ M was obtained from 8 point titration using Sigmaplot 9.0, where each individual point was an average of duplicate determination at the same concentration from three independent experiments. Note: Glutamate at 75 μ M increased the activity of NOS by 2.7 \pm 0.37-fold of the basal level.

MOL #29108

TABLE 3

Selective inhibition of nNOS by bis(7)-tacrine *in vitro*

Drug	IC ₅₀ (μM)		
	nNOS	iNOS	eNOS
Bis(7)-tacrine	2.9 ± 0.21	9.3 ± 0.59	>100
L-NMMA	4.1 ± 0.17	15.0 ± 0.37	3.8 ± 0.41
7-NI	0.7 ± 0.19	27.7 ± 0.76	1.9 ± 0.35
MK-801	-----ND*-----		
Memantine	-----ND-----		

In vitro, the activity of the recombinant human nNOS, eNOS and iNOS and their inhibition by chemicals were measured by the NOS assay kit as described in the Materials and Methods section. IC₅₀ value of each chemical to inhibit nNOS, iNOS and eNOS was obtained from 8 point titration using Sigmaplot 9.0, where each individual point was an average of duplicate determination at the same concentration from three independent experiments. *ND means 'not detectable', which indicate that the corresponding chemical does not inhibit the activity of NOS even at 1 mM.

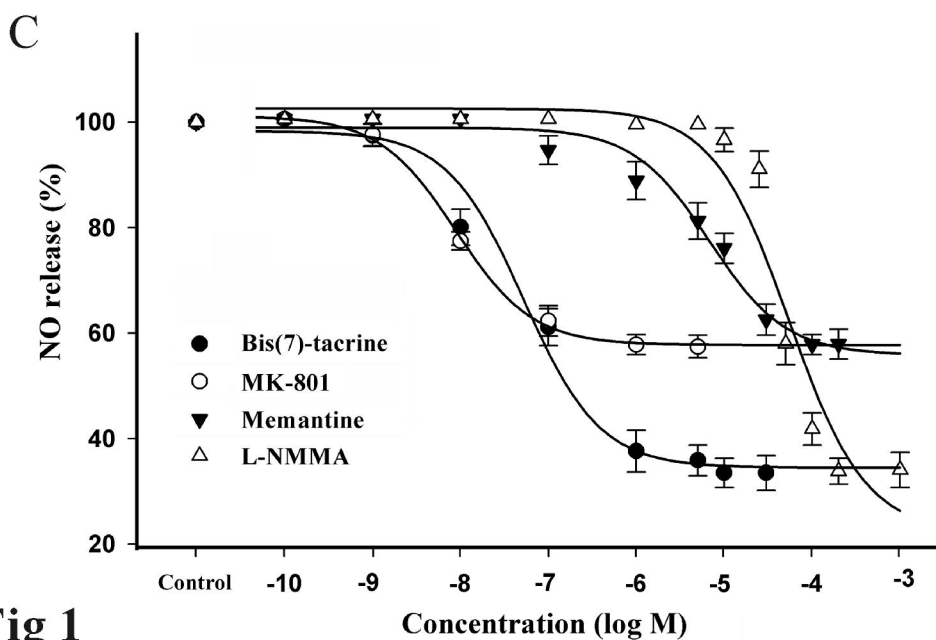
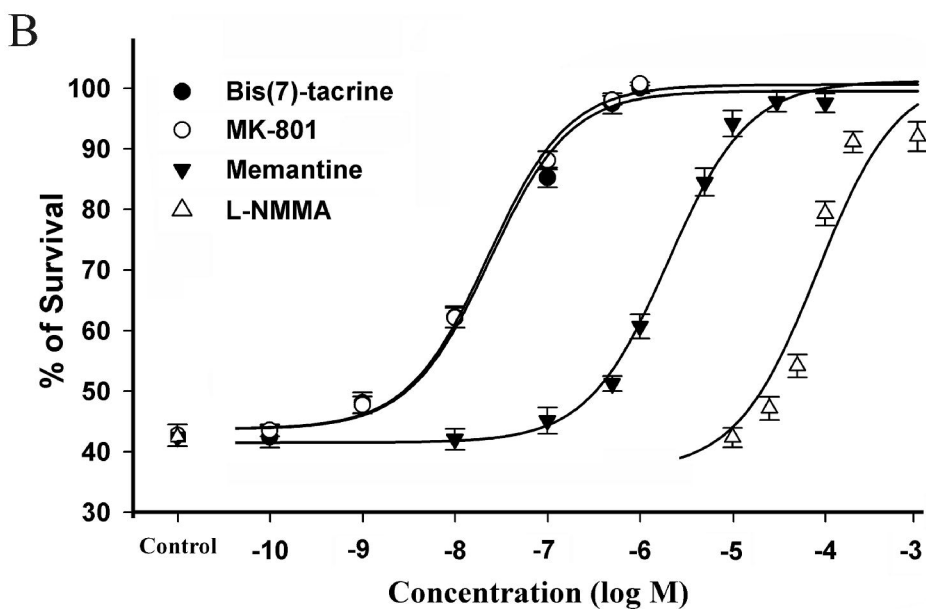
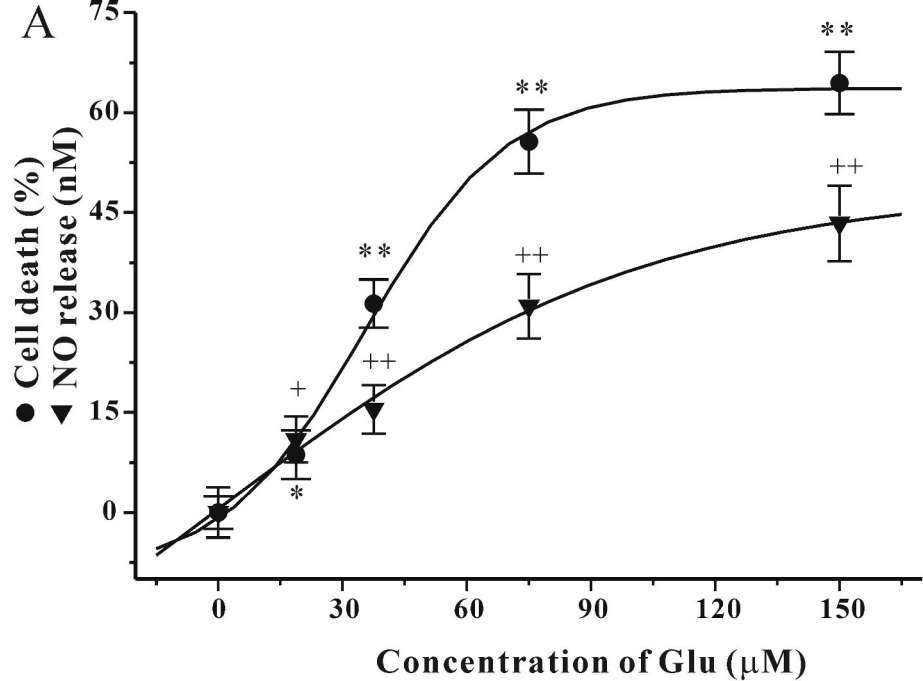


Fig 1

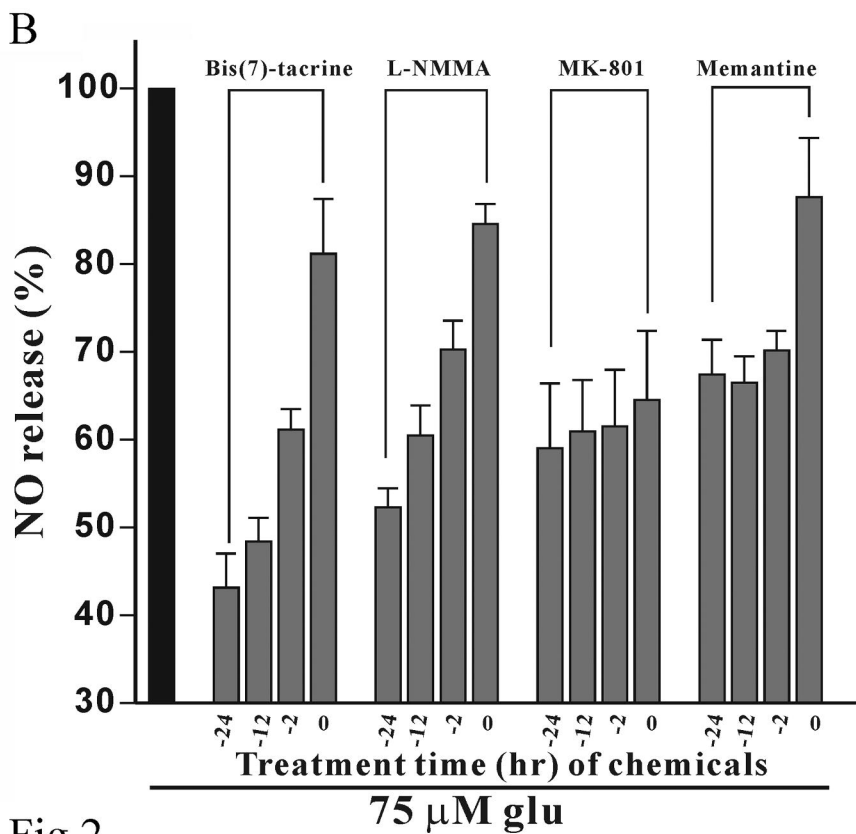
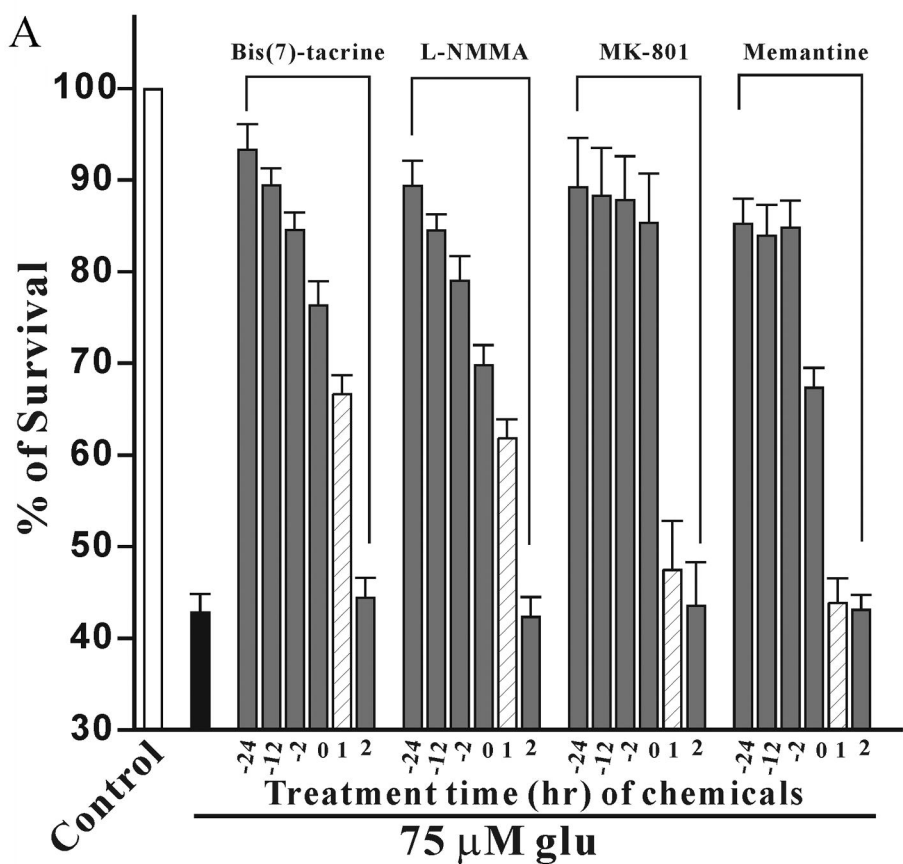


Fig 2

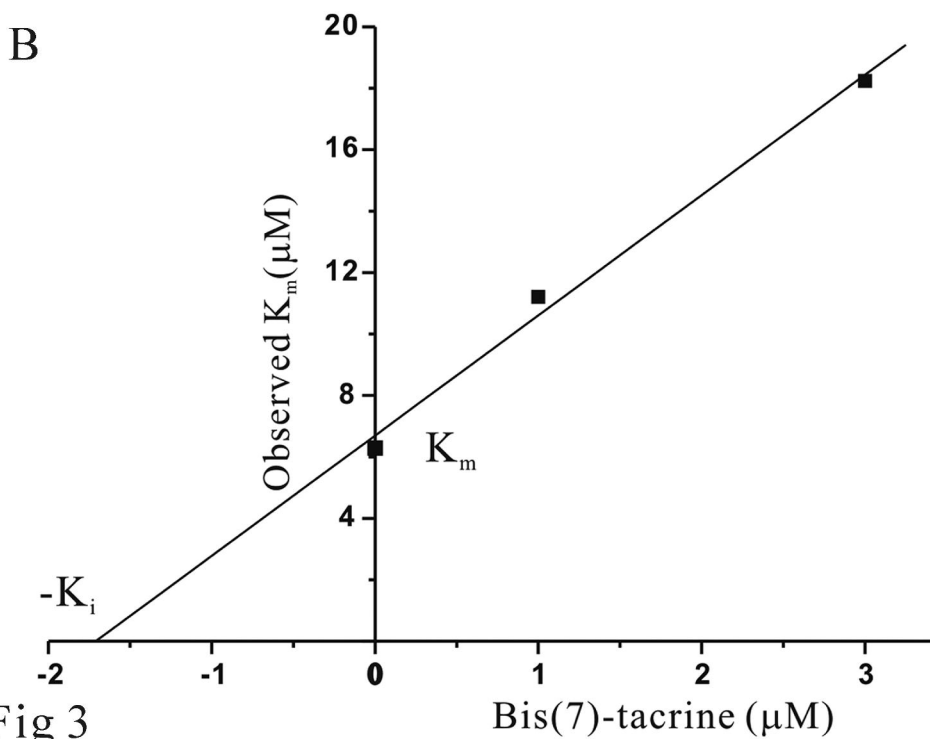
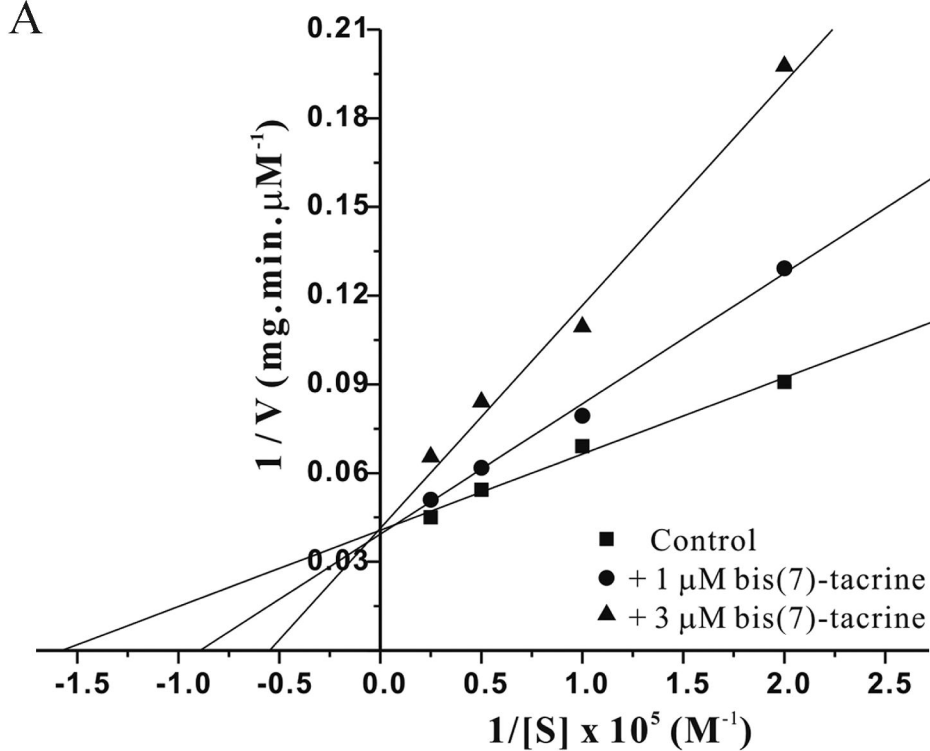
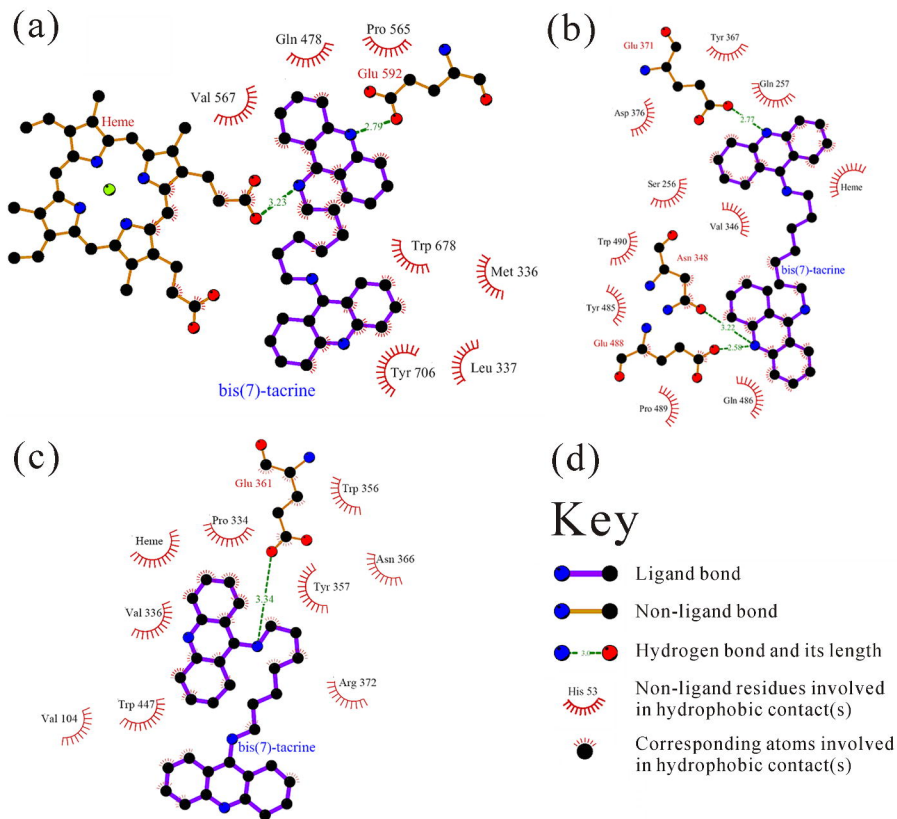


Fig 3

A



B

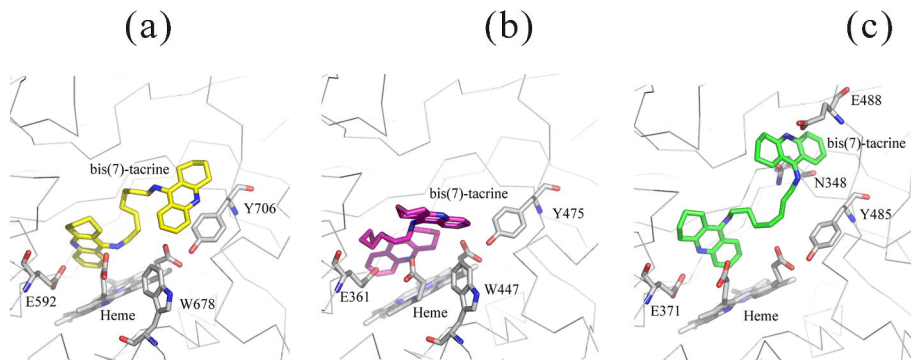


Fig 4

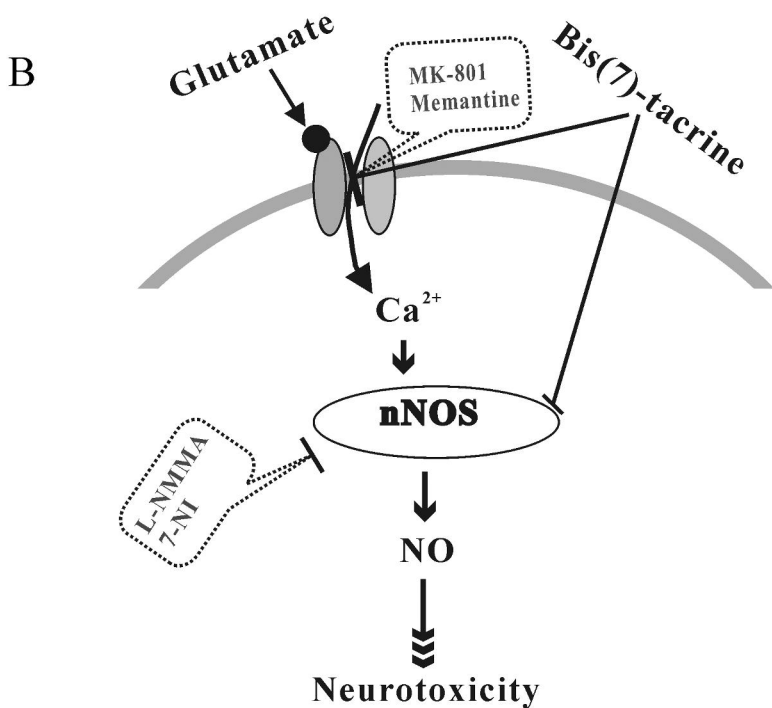
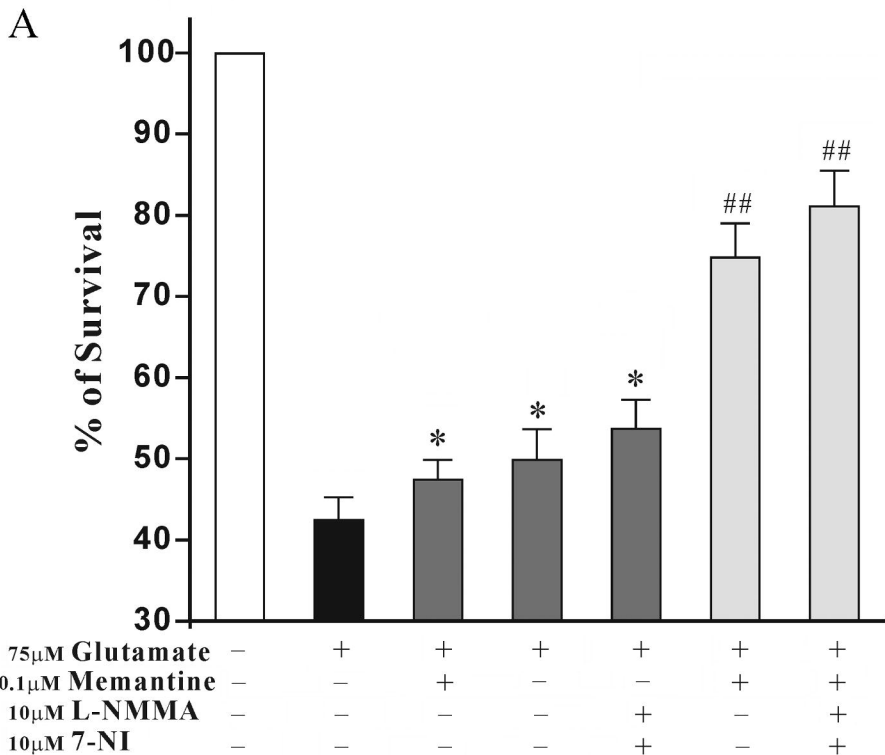


Fig 5